Vector meson photoproduction studied in its radiative decay channel

Qiang Zhao,[1,*] J. S. Al-Khalili,[1,†] and P. L. Cole[2,‡]
[1]*Department of Physics, University of Surrey, Guildford, Surrey GU2 7XH, United Kingdom*
[2]*Department of Physics, Idaho State University, Pocatello, Idaho 83209*
(Received 20 January 2005; published 24 May 2005)

We provide an analysis of vector meson photoproduction in the channel of the vector meson decaying into a pseudoscalar meson plus a photon (i.e., $V \to P\gamma$). It is shown that nontrivial kinematic correlations arise from the measurement of the $P\gamma$ angular distributions in the overall c.m. system in comparison with those in the vector meson rest frame. The implication of such kinematic correlations in the measurement of polarization observables is discussed in terms of the vector meson density matrix elements. For ω meson production, because of its relatively large branching ratios for $\omega \to \pi^0\gamma$, additional events from this channel may enrich the information about the reaction mechanism and improve the statistics of the recent measurement of polarized beam asymmetries by the GRAAL Collaboration. For $\phi \to \eta\gamma$, $\rho \to \pi\gamma$, and $K^* \to K\gamma$, we expect that additional information about the spin structure of the vector meson production vertex can be derived.

DOI: 10.1103/PhysRevC.71.054004 PACS number(s): 24.70.+s, 25.20.Lj, 13.88.+e, 13.20.−v

I. INTRODUCTION

In recent years direct experimental evidence has been sought for baryon resonance couplings into vector mesons in vector meson photoproduction reactions [1–4]. One of the motivations behind this effort is to find "missing resonances," which are predicted by the nonrelativistic constituent quark model (NRCQM) but are not found in πN scattering [5,6]. The study of vector meson photoproduction at large angles near threshold is particularly useful owing of the relatively small contributions from background processes, such as t-channel natural and unnatural parity exchanges.

Various experimental projects have been and are being carried out at ELSA, JLab, ESRF, and Spring-8. In addition to the cross sections, polarization observables, which are more sensitive to resonance excitations, will also be measured using newly developed experimental techniques [7,8]. This is of great importance for the purpose of disentangling the s-channel resonance excitations in the reaction. Because a large number of degrees of freedom will be involved and dynamic information in such a nonperturbative region is lacking, one, in principle, needs a complete set of measurements of all independent spin polarization observables to obtain sufficient information about resonance excitations and their couplings to the meson and nucleon [9].

The polarization observables and density matrix elements are essentially equivalent languages that connect the theoretical phenomenologies with the experimental observables. The density matrix elements, as the interference between the independent transition amplitudes, can be measured in the final state vector meson decay distributions. They can be directly compared with theoretical calculations, and hence they give access to dynamical information about the transition mechanism. For the vector meson photoproduction reaction, a number of analyses have been carried out in the literature. Density matrix elements for polarized photon beams were discussed by Schilling, Seyboth, and Wolf [10]. More recently, Pichowsky, Şavklı, and Tabakin [9] studied various relations between polarization observables and helicity amplitudes. In Refs. [11,12], Kloet *et al.* investigated inequality constraints on the density matrix elements defined for the produced vector meson with unpolarized or linearly polarized photon beams. They also explored relations between vector meson decay distributions in the vector meson rest frame and the overall γN frame, which can be extended to the analysis of other decay channels.

Another aspect relevant to the derivation of the density matrix elements is the dynamics for the produced vector meson coupling to the detected particles. For instance, the ω meson is usually detected in $\omega \to \pi^+\pi^-\pi^0$ and the ρ^0 in $\rho^0 \to \pi^+\pi^-$. The angular distributions for vector meson decays into spinless particles were studied in Ref. [10]. However, their decays into a photon and a pseudoscalar meson, $V \to P\gamma$, have not been discussed. In this work, we will develop the formalism for vector meson decay into a photon and a pseudoscalar meson (e.g., $\omega \to \pi^0\gamma$, $\phi \to \eta\gamma$, $\rho \to \pi\gamma$, and $K^* \to K\gamma$). We will show that additional information about the vector meson production mechanism can be obtained from measurements of those final states. This analysis has an advantage in ω meson photoproduction, for which the branching ratio of $\omega \to \pi^0\gamma$ is about 8.5% [13]. Because the ω meson is an isoscalar meson, only nucleon resonances can contribute in its s- and u-channel production. This significantly reduces the number of excited states in the corresponding reaction channels. In this sense, the additional information from $\omega \to \pi^0\gamma$ should be useful for constraining the nucleon resonances in $\gamma N \to \omega N$. Nevertheless, since the ω decays are dominantly via $\omega \to \pi^+\pi^-\pi^0$, and $\pi^+\pi^-$ could form a configuration of $J^P = 1^-$ as a photon, it is interesting to compare these two distributions and gain some insight into the sensitivities of the vector meson production mechanism to these two decay channels in a polarization measurement. This possibility is enhanced in the comparison between $V \to PP$ and $V \to P\gamma$. For $\phi \to \eta\gamma$,

*Electronic address: qiang.zhao@surrey.ac.uk
†Electronic address: j.al-khalili@surrey.ac.uk
‡Electronic address: cole@physics.isu.edu

the branching ratio is still sizeable. In comparison with the dominant decay channel of $\phi \to K\bar{K}$, the decay distribution of $\phi \to \eta\gamma$ contains different spin structure information; hence it should be more sensitive to the production mechanism. A similar feature, applies to the $\rho \to \pi\gamma$ and $K^* \to K\gamma$ in ρ and K^* meson photoproduction, respectively.

In this paper, the analysis of the decay channel $V \to P\gamma$ will be presented in Sec. II. In Sec. III, we discuss the kinematic correlations arising from this decay channel and analyze their influence on the measurements of spin observables in the the overall γN c.m. system. Comparison with the results derived in the vector meson rest frame will then be made. A summary will be given in Sec. IV. To make it convenient for readers, analyses of the spin observables in terms of the density matrix elements of the polarized particles are included in the Appendix.

II. DENSITY MATRIX ELEMENTS FOR $V \to P\gamma$

In the overall c.m. system, the invariant amplitude is defined as

$$T_{\lambda_v\lambda_f,\lambda_\gamma\lambda_i} \equiv \langle \mathbf{q}, \lambda_v; \mathbf{P}_f, \lambda_f | T | \mathbf{k}, \lambda_\gamma; \mathbf{P}_i, \lambda_i \rangle \to \langle \lambda_v\lambda_f | T | \lambda_\gamma\lambda_i \rangle, \quad (1)$$

where $\mathbf{k}$ and $\mathbf{q}$ are momenta of the initial photon and final state vector meson, respectively; momenta $\mathbf{P}_i = -\mathbf{k}$ and $\mathbf{P}_f = -\mathbf{q}$ are for the initial and final state nucleons, respectively; and λ_γ $(= \pm 1)$, λ_v $(= 0, \pm 1)$, λ_i $(= \pm 1/2)$, and λ_f $(= \pm 1/2)$ are helicities of the photon, vector meson, and initial and final state nucleons, respectively.

The amplitudes for the two photon polarizations $\lambda_\gamma = \pm 1$ are not independent of each other. They are connected by the Jacob-Wick parity relation:

$$\langle \lambda_v\lambda_f | T | \lambda_\gamma\lambda_i \rangle = (-1)^{(\lambda_v-\lambda_f)-(\lambda_\gamma-\lambda_i)} \times \langle -\lambda_v - \lambda_f | T | -\lambda_\gamma - \lambda_i \rangle. \quad (2)$$

We first consider the vector meson decay in the overall γN c.m. system. The decay of vector meson ($J^{PC} = 1^-$) into a pseudoscalar meson ($J^P = 0^-$) and photon ($J^{PC} = 1^{--}$) (i.e., $V \to P\gamma$) is described by the effective Lagrangian

$$\mathcal{L}_{VP\gamma} = \frac{eg_V}{M_V} \epsilon_{\alpha\beta\gamma\delta} \partial^\alpha A^\beta \partial^\gamma V^\delta P, \quad (3)$$

where g_V is the coupling constant and $\epsilon_{\alpha\beta\gamma\delta}$ is the Levi-Civita tensor; V^δ and P here denote the vector and pseudoscalar meson fields, and A^β is the photon field. This effective Lagrangian is the only Lorentz-covariant one for the $VP\gamma$ coupling at leading order.

We assume that the fields couple as elementary ones. Therefore, the momentum dependence of g_V can be neglected [i.e., $g_V = g_V(0)$]. This assumption depends on the average radius $\langle r_q^2 \rangle^{1/2}$ of the vector meson, for which we phenomenologically refer to the average distance between the quark and antiquark within the meson. As a simple estimate for the ground-state mesons of which the spatial wave functions are spherical, the particle size effects appear as the quadratic term in the form factor $1 - k_q^2 \langle r_q^2 \rangle / 6$, where $k_q \simeq 380$ MeV are the typical constituent quark momenta. For a typical meson size of $\langle r_q^2 \rangle^{1/2} \sim 0.5$ fm, a correction of about 15% seems to be needed. However, this will not affect the general feature of the subsequent analyses for two reasons: (i) As shown by Becchi and Morpurgo [14], in the limit of $k_q = 0$ [i.e., $g_V(k_q^2) = g_V(0)$], the calculations for both limits of $M_V = M_P(\text{exp})$ and $M_P = M_V(\text{exp})$ give the same results, which are consistent with the experimental data. This suggests that the momentum dependence of g_V is not significant. (ii) Even though $g_V(k_q^2) \neq g_V(0)$, this only leads to some percentage of descrepancies in the event counting between the calculation of Eq. (3) and experimental statistics, whereas the decay distributions will not change. In this sense, we can neglect the momentum dependence of g_V at this moment, and focus on the study of kinematic correlations arising from the measurement of the $P\gamma$ angular distributions.

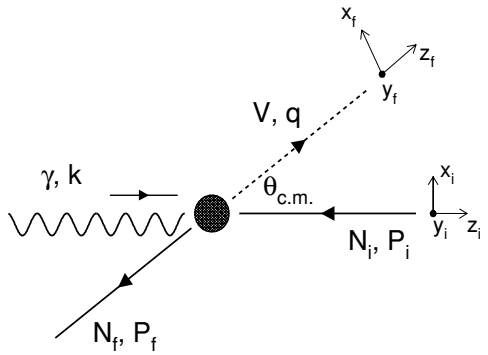

FIG. 1. Kinematics for $\gamma N_i \to V N_f$ in the overall c.m. system.

It is worth noting that the vector meson size effects may become non-negligible at the production vertices for $\gamma N \to VN$, and careful considerations of the vector meson coupling form factors are crucial. However, this is independent of our motivation here. As mentioned in the Introduction, we are interested in possible experimental measurements of the angular distributions of final state particles, through which dynamical information about the production mechanism (contained in the density matrix elements) can be extracted.

As illustrated in Fig. 1, we define the z_f axis along the three moment of the vector meson, the y_f axis is normal to the production plane defined by $\mathbf{k} \times \mathbf{q}$, and hence the x_f direction is determined by $y_f \times z_f$. Since the vector meson three momentum $|\mathbf{q}|$ is determined by the c.m. energy W, the three momentum of the final state photon in the overall c.m. system can be expressed as $\mathbf{p} = \mathbf{q}/2 + \mathbf{r}$, where $\mathbf{r}$ is the three momentum of the photon in the vector meson rest frame. The z_f axis also defines the z direction of the decay coordinates; the polar angle θ and azimuthal angle ϕ are defined by the momentum difference between the final-state photon and pseudoscalar meson, $\mathbf{p} - \mathbf{p_s} = 2\mathbf{r}$. However, for the description of vector meson decay, it is convenient to select the decay angles, θ_c and ϕ_c, which are the polar and azimuthal angles of the flight direction of the photon in the overall c.m. system with respect to z_f. As shown in Fig. 2, we have

$$\begin{aligned} p_0 \sin\theta_c &= |\mathbf{r}| \sin\theta, \\ p_0 \cos\theta_c &= |\mathbf{r}| \cos\theta + |\mathbf{q}|/2, \\ \phi_c &= \phi, \end{aligned} \quad (4)$$

where $p_0 = |\mathbf{p}|$ is the energy of the final-state photon.

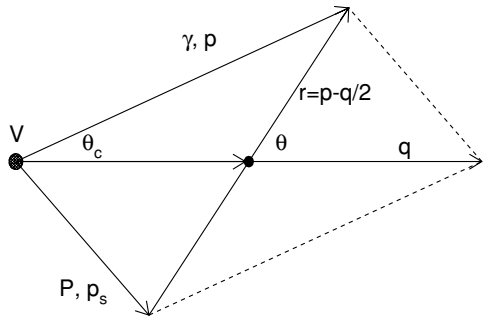

FIG. 2. Kinematics for $V \to P\gamma$ in the overall c.m. system where the vector meson has momentum $\mathbf{q}$. The angle θ_c denotes the decay direction of the photon; θ is the angle between $\mathbf{q}$ and the momentum difference between the photon and pseudoscalar meson.

The decay amplitude of the vector meson with transverse polarization can thus be expressed as

$$\begin{aligned}\langle \Lambda_\gamma; \theta_c, \phi_c | M | \lambda_v = \pm 1 \rangle &= C\sqrt{\frac{3}{8\pi}}\frac{p_0(q^0\Lambda_\gamma + |\mathbf{q}|\lambda_v)}{M_V}\boldsymbol{\epsilon}_\gamma \cdot \boldsymbol{\epsilon}_v \\ &= C\sqrt{\frac{3}{8\pi}}\frac{p_0(q^0\Lambda_\gamma + |\mathbf{q}|\lambda_v)}{M_V}(-1)^{\lambda_v} \\ &\quad \times D^{1*}_{-\lambda_v \Lambda_\gamma}(\phi_c, \theta_c, -\phi_c), \end{aligned} \tag{5}$$

and the amplitude with longitudinal polarization is

$$\begin{aligned}\langle \Lambda_\gamma; \theta_c, \phi_c | M | \lambda_v = 0 \rangle &= C\sqrt{\frac{3}{8\pi}}|\mathbf{p}|\Lambda_\gamma \boldsymbol{\epsilon}_\gamma \cdot \hat{\mathbf{q}} \\ &= C\sqrt{\frac{3}{8\pi}}|\mathbf{p}|\Lambda_\gamma D^{1*}_{0\Lambda_\gamma}(\phi_c, \theta_c, -\phi_c), \end{aligned} \tag{6}$$

where $\Lambda_\gamma = \pm 1$ and $\lambda_v = 0, \pm 1$ are the helicities of the photon and vector meson in $V \to P\gamma$, respectively. The coefficient $C = eg_V$ is the coupling constant.

The Wigner rotation functions follow the convention of Rose [15]:

$$D^I_{\mathrm{MN}}(\alpha, \beta, \gamma) = e^{-i(M\alpha + N\gamma)} d^I_{\mathrm{MN}}(\beta), \tag{7}$$

where α, β, and γ are Euler angles for the rotations of a vector.

Similar to the case of a vector meson decaying into spinless particles [10], we can express the angular distribution of $V \to P\gamma$ in terms of the vector meson density matrix elements $\rho_{\lambda_v \lambda'_v}$:

$$\begin{aligned}\frac{dN}{d\cos\theta d\phi} &= W(\cos\theta_c, \phi_c, \rho) \\ &= W_{\mathrm{TT}}(\cos\theta_c, \phi_c, \rho) + W_{\mathrm{LL}}(\cos\theta_c, \phi_c, \rho) \\ &\quad + W_{\mathrm{TL}}(\cos\theta_c, \phi_c, \rho), \end{aligned} \tag{8}$$

where θ_c and ϕ_c are functions of θ and ϕ; and the latter angles (θ, ϕ) are the variables of the differential distributions on the left-hand side; the subscripts TT, LL, and TL denote the interfering distribution functions between the transverse-transverse, longitudinal-longitudinal, and transverse-longitudinal vector meson polarizations, respectively.

These have the following expressions in the overall c.m. system:

$$\begin{aligned} W_{\mathrm{TT}}(\cos\theta_c, \phi_c, \rho) &= \frac{1}{\sigma_0}\sum_{\lambda_v, \lambda'_v = \pm 1; \Lambda_\gamma, \Lambda'_\gamma} \langle \Lambda_\gamma; \theta, \phi | M | \lambda_v \rangle \\ &\quad \times \rho_{\lambda_v \lambda'_v}\delta_{\Lambda_\gamma \Lambda'_\gamma}\langle \lambda'_v | M^\dagger | \Lambda'_\gamma; \theta, \phi \rangle \\ &= \frac{C^2}{\sigma_0}\frac{3}{8\pi}\sum_{\lambda_v, \lambda'_v = \pm 1; \Lambda_\gamma}\frac{p_0(q_0\Lambda_\gamma + |\mathbf{q}|\lambda_v)}{M_V} \\ &\quad \times (-1)^{\lambda_v} D^{1*}_{-\lambda_v \Lambda_\gamma}(\phi_c, \theta_c, -\phi_c)\rho_{\lambda_v \lambda'_v}(V) \\ &\quad \times (-1)^{\lambda'_v} D^{1}_{-\lambda'_v \Lambda'_\gamma}(\phi_c, \theta_c, -\phi_c) \\ &\quad \times \frac{p_0(q_0\Lambda'_\gamma + |\mathbf{q}|\lambda'_v)}{M_V} \\ &= \frac{C^2}{\sigma_0}\frac{3}{8\pi}\frac{p_0^2}{2}\left\{\left[\mathcal{F}_1^2(\theta_c) + \mathcal{F}_2^2(\theta_c)\right]\right. \\ &\quad \times (\rho_{11} + \rho_{-1-1}) + \sin^2\theta_c \\ &\quad \left. \times [e^{-2i\phi_c}\rho_{1-1} + e^{2i\phi_c}\rho_{-11}]\right\}, \end{aligned} \tag{9}$$

$$\begin{aligned} W_{\mathrm{LL}}(\cos\theta_c, \phi_c, \rho) &= \frac{C^2}{\sigma_0}\frac{3}{8\pi}\sum_{\lambda_v = \lambda'_v = 0; \Lambda_\gamma, \Lambda'_\gamma}|\mathbf{p}|^2 \Lambda_\gamma \Lambda'_\gamma D^{1*}_{0\Lambda_\gamma} \\ &\quad \times (\phi_c, \theta_c, -\phi_c)\delta_{\Lambda_\gamma \Lambda'_\gamma}\rho_{00}(V)D^1_{0\Lambda'_\gamma} \\ &\quad \times (\phi_c, \theta_c, -\phi_c) \\ &= \frac{C^2}{\sigma_0}\frac{3}{8\pi}|\mathbf{p}|^2 \sin^2\theta_c \rho_{00}, \end{aligned} \tag{10}$$

and

$$\begin{aligned} W_{\mathrm{TL}}(\cos\theta_c, \phi_c, \rho) &= \frac{C^2}{\sigma_0}\frac{3}{8\pi}\sum_{\lambda_v, \lambda'_v \neq 0; \Lambda_\gamma}\frac{p_0|\mathbf{p}|\Lambda_\gamma}{M_V} \\ &\quad \times \left[(q_0\Lambda_\gamma + |\mathbf{q}|\lambda_v)(-1)^{\lambda_v} D^{1*}_{-\lambda_v \Lambda_\gamma}\right. \\ &\quad \times (\phi_c, \theta_c, -\phi_c)\rho_{\lambda_v 0} D^1_{0\Lambda_\gamma}(\phi_c, \theta_c, -\phi_c) \\ &\quad + (q_0\Lambda_\gamma + |\mathbf{q}|\lambda'_v)(-1)^{\lambda'_v} D^{1*}_{0\Lambda_\gamma} \\ &\quad \times (\phi_c, \theta_c, -\phi_c)\rho_{0\lambda'_v} D^1_{-\lambda'_v \Lambda_\gamma} \\ &\quad \left. \times (\phi_c, \theta_c, -\phi_c)\right] \\ &= -\frac{C^2}{\sigma_0}\frac{3}{8\pi}\frac{p_0^2 \sin\theta_c}{2\sqrt{2}}[\mathcal{F}_1(\theta_c) - \mathcal{F}_2(\theta_c)] \\ &\quad \times [e^{-i\phi_c}(\rho_{10} - \rho_{0-1}) + e^{i\phi_c} \\ &\quad \times (\rho_{01} - \rho_{-10})], \end{aligned} \tag{11}$$

where

$$\begin{aligned} \mathcal{F}_1(\theta_c) &\equiv \frac{1}{M_V}(q_0 + |\mathbf{q}|)(1 - \cos\theta_c), \\ \mathcal{F}_2(\theta_c) &\equiv \frac{1}{M_V}(q_0 - |\mathbf{q}|)(1 + \cos\theta_c) \end{aligned} \tag{12}$$

are functions of θ_c and hence introduce kinematic correlations to the coordinate transformation. The δ function $\delta_{\Lambda_\gamma \Lambda'_\gamma}$ implies the sum over the final-state unpolarized photons. The factor $\sigma_0 = C^2|\mathbf{r}|^2$ is the normalization factor for $V \to P\gamma$ and is proportional to the decay width for $V \to P\gamma$ in the vector

meson rest frame. Note that $W(\cos\theta_c, \phi_c, \rho)$ is coordinate dependent owing to the Lorentz transformation from the vector meson rest frame to the overall c.m. system.

The density matrix elements of the vector meson are independent of the coordinate frame selection for the vector meson decays. They are related to the initial photon polarizations in the overall c.m. system via

$$\rho_{\lambda_v\lambda'_v}(V) = \frac{1}{N}\sum_{\lambda_f\lambda_\gamma\lambda_i\lambda'_\gamma} T_{\lambda_v\lambda_f,\lambda_\gamma\lambda_i}\rho_{\lambda_\gamma\lambda'_\gamma}(\gamma)T^*_{\lambda'_v\lambda_f,\lambda'_\gamma\lambda_i}, \quad (13)$$

where $N \equiv \frac{1}{2}\sum_{\lambda_v\lambda_f\lambda_\gamma\lambda_i}|T_{\lambda_v\lambda_f,\lambda_\gamma\lambda_i}|^2$ is the normalization factor and is double the unpolarized cross section if one ignores the phase space factor.

The polarized-photon density matrix element $\rho(\gamma)$ is defined as [10]

$$\rho(\gamma) = \tfrac{1}{2}(I_\gamma + \boldsymbol{\sigma}\cdot\mathbf{P}_\gamma), \quad (14)$$

where $\boldsymbol{\sigma}$ is the Pauli matrix for the photon's two independent polarizations; $\mathbf{P}_\gamma$ determines both the degree of polarization (via its magnitude P_γ) and the polarization direction. For linearly polarized photons, with Φ denoting the angle between the polarization vector of the photon $(\cos\Phi, \sin\Phi, 0)$ and the production plane ($x_i - z_i$ plane), one has $\mathbf{P}_\gamma = P_\gamma(-\cos 2\Phi, -\sin 2\Phi, 0)$. For circularly polarized photons, the polarization vector is along the z_i axis and hence $\mathbf{P}_\gamma = P_\gamma(0, 0, \lambda_\gamma)$ with $\lambda_\gamma = \pm 1$.

Substituting Eq. (14) into (13), we obtain the familiar form of the vector meson density matrix elements [10]:

$$\begin{aligned}
\rho^0_{\lambda_v\lambda'_v} &= \frac{1}{2N}\sum_{\lambda_\gamma\lambda_f\lambda_i} T_{\lambda_v\lambda_f,\lambda_\gamma\lambda_i}T^*_{\lambda'_v\lambda_f,\lambda_\gamma\lambda_i},\\
\rho^1_{\lambda_v\lambda'_v} &= \frac{1}{2N}\sum_{\lambda_\gamma\lambda_f\lambda_i} T_{\lambda_v\lambda_f,-\lambda_\gamma\lambda_i}T^*_{\lambda'_v\lambda_f,\lambda_\gamma\lambda_i},\\
\rho^2_{\lambda_v\lambda'_v} &= \frac{i}{2N}\sum_{\lambda_\gamma\lambda_f\lambda_i} \lambda_\gamma T_{\lambda_v\lambda_f,-\lambda_\gamma\lambda_i}T^*_{\lambda'_v\lambda_f,\lambda_\gamma\lambda_i},\\
\rho^3_{\lambda_v\lambda'_v} &= \frac{i}{2N}\sum_{\lambda_\gamma\lambda_f\lambda_i} \lambda_\gamma T_{\lambda_v\lambda_f,\lambda_\gamma\lambda_i}T^*_{\lambda'_v\lambda_f,\lambda_\gamma\lambda_i}.
\end{aligned} \quad (15)$$

The decomposition of the vector meson decay distribution in terms of the initial photon polarizations thus allows us to express Eq. (8) as

$$\begin{aligned}
W(\cos\theta_c, \phi_c, \rho) = {} & W^0(\cos\theta_c, \phi_c, \rho^0)\\
& + \sum_{\alpha=1}^{3} P^\alpha_\gamma W^\alpha(\cos\theta_c, \phi_c, \rho^\alpha),
\end{aligned} \quad (16)$$

where W^0 denotes the distribution with unpolarized photons, $W^{1,2}$ denote those with linearly polarized photons, and W^3 denotes that with circularly polarized photons.

With the Jacob-Wick parity relation [Eq. (2)] and the requirement that the density matrix elements must be Hermitian,

$$\rho^\alpha_{\lambda_v\lambda'_v} = \rho^{\alpha *}_{\lambda'_v\lambda_v}, \quad (17)$$

the decomposed distributions can be obtained:

$$\begin{aligned}
W^0(\cos\theta_c, \phi_c, \rho^0) = {} & \frac{3}{8\pi}\frac{C^2p_0^2}{\sigma_0}\Big\{\sin^2\theta_c\rho^0_{00} + \frac{1}{2}\big[\mathcal{F}_1^2(\theta_c)\\
& + \mathcal{F}_2^2(\theta_c)\big]\rho^0_{11} + \sin^2\theta_c\cos 2\phi_c\rho^0_{1-1}\\
& + \sqrt{2}[\mathcal{F}_1(\theta_c) - \mathcal{F}_2(\theta_c)]\\
& \times \sin\theta_c\cos\phi_c\ \mathrm{Re}\ \rho^0_{10}\Big\},
\end{aligned} \quad (18)$$

$$\begin{aligned}
W^1(\cos\theta_c, \phi_c, \rho^0) = {} & \frac{3}{8\pi}\frac{C^2p_0^2}{\sigma_0}\Big\{\sin^2\theta_c\rho^1_{00} + \frac{1}{2}\big[\mathcal{F}_1^2(\theta_c)\\
& + \mathcal{F}_2^2(\theta_c)\big]\rho^1_{11} + \sin^2\theta_c\cos 2\phi_c\rho^1_{1-1}\\
& + \sqrt{2}[\mathcal{F}_1(\theta_c) - \mathcal{F}_2(\theta_c)]\\
& \times \sin\theta_c\cos\phi_c\ \mathrm{Re}\ \rho^1_{10}\Big\},
\end{aligned} \quad (19)$$

$$\begin{aligned}
W^2(\cos\theta_c, \phi_c, \rho^2) = {} & \frac{3}{8\pi}\frac{C^2p_0^2}{\sigma_0}\big\{\sin^2\theta_c\sin 2\phi_c\mathrm{Im}\,\rho^2_{1-1}\\
& - \sqrt{2}[\mathcal{F}_1(\theta_c) - \mathcal{F}_2(\theta_c)]\\
& \times \sin\theta_c\sin\phi_c\ \mathrm{Im}\ \rho^2_{10}\big\},
\end{aligned} \quad (20)$$

and

$$\begin{aligned}
W^3(\cos\theta_c, \phi_c, \rho^2) = {} & \frac{3}{8\pi}\frac{C^2p_0^2}{\sigma_0}\big\{\sin^2\theta_c\sin 2\phi_c\mathrm{Im}\,\rho^3_{1-1}\\
& - \sqrt{2}[\mathcal{F}_1(\theta_c) - \mathcal{F}_2(\theta_c)]\\
& \times \sin\theta_c\sin\phi_c\ \mathrm{Im}\ \rho^3_{10}\big\}.
\end{aligned} \quad (21)$$

Recalling again that θ_c is a function of θ, we see that strong kinematic correlations have been embedded in these expressions. Naturally, one would expect that in the limit of $|\mathbf{q}| \to 0$, and hence $q_0 \to M_V$, the azimuthal angles (θ_c, ϕ_c) will be identical to (θ, ϕ), and $C^2p_0^2/\sigma_0 = p_0^2/|\mathbf{r}|^2 = 1$. These expressions then reduce to the ones derived in the vector meson rest frame [10]:

$$\begin{aligned}
W^0(\cos\theta, \phi, \rho^0) = {} & \frac{3}{8\pi}\big\{\sin^2\theta\rho^0_{00} + (1 + \cos^2\theta)\rho^0_{11}\\
& + \sin^2\theta\cos 2\phi\rho^0_{1-1}\\
& + \sqrt{2}\sin 2\theta\cos\phi\ \mathrm{Re}\ \rho^0_{10}\big\},
\end{aligned} \quad (22)$$

$$\begin{aligned}
W^1(\cos\theta, \phi, \rho^1) = {} & \frac{3}{8\pi}\big\{\sin^2\theta\rho^1_{00} + (1 + \cos^2\theta)\rho^1_{11}\\
& + \sin^2\theta\cos 2\phi\rho^1_{1-1}\\
& + \sqrt{2}\sin 2\theta\cos\phi\ \mathrm{Re}\ \rho^1_{10}\big\},
\end{aligned} \quad (23)$$

$$\begin{aligned}
W^2(\cos\theta, \phi, \rho^2) = {} & \frac{3}{8\pi}\big\{\sin^2\theta\sin 2\phi\ \mathrm{Im}\ \rho^2_{1-1}\\
& + \sqrt{2}\sin 2\theta\sin\phi\ \mathrm{Im}\ \rho^2_{10}\big\},
\end{aligned} \quad (24)$$

and

$$\begin{aligned}
W^3(\cos\theta, \phi, \rho^3) = {} & \frac{3}{8\pi}\big\{\sin^2\theta\sin 2\phi\ \mathrm{Im}\ \rho^3_{1-1}\\
& + \sqrt{2}\sin 2\theta\sin\phi\ \mathrm{Im}\ \rho^3_{10}\big\}.
\end{aligned} \quad (25)$$

As shown in Eq. (5), the nonvanishing three momentum of the vector meson in the overall c.m. system introduces an additional term for the transverse vector meson decays. As a consequence, kinematic factors $\mathcal{F}_{1,2}(\theta_c)$, which are functions of the decay angle θ_c, appear in the TT and TL decay distributions. Nevertheless, coordinate transformations also exist between θ_c and θ. In comparison with Eqs. (22–25) for vector meson decay in its rest frame, kinematic factors in Eqs. (18–21) cannot be cleanly factored out in the measurement of $V \to P\gamma$ in the overall c.m. system. This differs from the measurement of vector meson decay into spinless mesons [11] (e.g., $\rho^0 \to \pi^+\pi^-$ or $\phi \to K^+K^-$), where a kinematic factor can be taken out of the distribution functions by selecting the polar angle θ as the angle between the momentum difference of the final-state pions and the vector meson momentum in the overall c.m. system. Such a correlation also reflects the dynamical difference between $V \to P\gamma$ and $V \to PP$, from which we expect to learn more about the vector meson production mechanism via the measurement of the decay distributions.

In the next section, we will discuss some features arising from the kinematic correlations and their impact on the polarized beam asymmetry measurement in different frames.

III. KINEMATIC CORRELATIONS IN POLARIZED BEAM ASYMMETRY

In the production plane, the measurement of the linearly polarized beam asymmetry is defined as the cross section difference between polarizing the photons along the x_i ($\Phi = 0^\circ$) and y_i axis ($\Phi = 90^\circ$), which correspond to $\mathbf{P}_\gamma$ along $\mp x_i$, respectively. The cross sections for these two polarizations thus can be expressed as

$$\begin{aligned}\bar{W}_\perp(\Phi = 90^\circ, \rho) &= \int_{\theta=0}^{\pi}\int_{\phi=0}^{2\pi} d\Omega W^0(\cos\theta_c, \phi_c, \rho^0) \\ &\quad - P_\gamma \int_{\theta=0}^{\pi}\int_{\phi=0}^{2\pi} d\Omega W^1(\cos\theta_c, \phi_c, \rho^1) \\ &= \bar{W}^0(\rho^0) + P_\gamma \bar{W}^1(\rho^1) \end{aligned} \tag{26}$$

and

$$\bar{W}_\parallel(\Phi = 0^\circ, \rho) = \bar{W}^0(\rho^0) - P_\gamma \bar{W}^1(\rho^1). \tag{27}$$

The linearly polarized photon asymmetry is thus defined as

$$\check{\Sigma} \equiv \frac{\bar{W}_\perp(\Phi = 90^\circ, \rho) - \bar{W}_\parallel(\Phi = 0^\circ, \rho)}{\bar{W}_\perp(\Phi = 90^\circ, \rho) + \bar{W}_\parallel(\Phi = 0^\circ, \rho)} = P_\gamma \frac{\bar{W}^1(\rho^1)}{\bar{W}^0(\rho^0)}, \tag{28}$$

where P_γ is determined by the experimental setup, and $\bar{W}^1(\rho^1)$ and $\bar{W}^0(\rho^0)$ are the integrals over (θ, ϕ):

$$\begin{aligned}\bar{W}^1(\rho^1) &\equiv \int d\Omega W^1(\cos\theta_c, \phi_c, \rho^1) \\ &= \frac{3}{8\pi}\frac{1}{|\mathbf{r}|^2 M_V^2}\int d\Omega \big\{\big[(p\cdot q)^2 - M_V^2\big(p\cdot\epsilon_v^0\big)^2\big]\rho_{00}^1 \\ &\quad + \big[(p\cdot q)^2 + M_V^2\big(p\cdot\epsilon_v^0\big)^2\big]\rho_{11}^1\big\} \end{aligned} \tag{29}$$

and

$$\begin{aligned}\bar{W}^0(\rho^0) &\equiv \int d\Omega W^0(\cos\theta_c, \phi_c, \rho^0) \\ &= \frac{3}{8\pi}\frac{1}{|\mathbf{r}|^2 M_V^2}\int d\Omega \big\{\big[(p\cdot q)^2 - M_V^2\big(p\cdot\epsilon_v^0\big)^2\big]\rho_{00}^0 \\ &\quad + \big[(p\cdot q)^2 + M_V^2\big(p\cdot\epsilon_v^0\big)^2\big]\rho_{11}^0\big\}, \end{aligned} \tag{30}$$

where the relation $p_0^2[\mathcal{F}_1^2(\theta_c) + \mathcal{F}_2^2(\theta_c)]/2 = [(p\cdot q)^2 + M_V^2(p\cdot\epsilon_v^0)^2]/M_V^2$ has been applied, and $\epsilon_v^0 = (|\mathbf{q}|, q_0\hat{\mathbf{q}})/M_V$ is the longitudinal polarization vector of the vector meson.

Note that the density matrix elements ρ^α ($\alpha = 0, 1, 2, 3$) are independent of θ and ϕ. We define the following two integrals:

$$\begin{aligned} W_a &\equiv \frac{3}{8\pi}\frac{1}{|\mathbf{r}|^2 M_V^2}\int d\Omega\big[(p\cdot q)^2 - M_V^2\big(p\cdot\epsilon_v^0\big)^2\big], \\ W_b &\equiv \frac{3}{8\pi}\frac{1}{|\mathbf{r}|^2 M_V^2}\int d\Omega\big[(p\cdot q)^2 + M_V^2\big(p\cdot\epsilon_v^0\big)^2\big]. \end{aligned} \tag{31}$$

Hence, the polarized beam asymmetry can be expressed as

$$\check{\Sigma} = \frac{\rho_{00}^1 + (W_b/W_a)\rho_{11}^1}{\rho_{00}^0 + (W_b/W_a)\rho_{11}^0}, \tag{32}$$

and the ratio of the integrals gives

$$\frac{W_b}{W_a} = 2 + \frac{1}{2}\frac{|\mathbf{q}|^2}{M_V^2}\left(1 + \frac{3}{2}\frac{M_P^2}{|\mathbf{r}|^2}\right), \tag{33}$$

where, in the integration, the relation $2q_0p_0 = q_0^2 + p_0^2 - M_P^2 - (\mathbf{r} - \mathbf{q}/2)^2$ has been used. In the vector meson rest frame, $|\mathbf{q}| \to 0$, we have $W_b/W_a = 2$, and the polarized beam asymmetry reduces to

$$\check{\Sigma} = \frac{\rho_{00}^1 + 2\rho_{11}^1}{\rho_{00}^0 + 2\rho_{11}^0}, \tag{34}$$

which is the familiar result derived for the vector meson decays into pseudoscalar mesons [16].

Because of the nontrivial kinematic correlations arising from the decay distributions, the polarized photon beam asymmetry is also accompanied by a kinematic correlation factor when transforming from the vector meson rest frame to the overall c.m. frame. Although one, in principle, can select the vector meson rest frame as the working frame for deriving the polarization asymmetry, in reality, it will depend on how well the vector meson kinematics is reconstructed. For narrow states, such as ω and ϕ, the transformation of the working frame from the overall c.m. one to the vector meson rest one should have relatively small ambiguities. However, for broad states, such as ρ, the sizeable width will lead to uncertainties in determining the three moment $\mathbf{q}$. The kinematic correlations hence will produce significant effects in the measurement of the polarization observables.

This kind of situation makes Eq. (34) useful for evaluating the kinematic correlation effects. First, note that the second term in Eq. (34) explicitly depends on the mass and momentum of the pseudoscalar meson in the vector meson rest frame. This shows that the kinematic correlations will become more significant if the vector meson decays into a heavier pseudoscalar meson instead of a lighter one owing of the

increasing ratio $M_P^2/|\mathbf{r}|^2$. For instance, for the final state decays of $\omega \to \eta\gamma$, $M_\pi^2/|\mathbf{r}_\pi|^2 = 0.13$, and for $\omega \to \pi^0\gamma$, $M_\eta^2/|\mathbf{r}_\eta|^2 = 7.56$. This ratio is essentially a constant for a fixed decay channel. Therefore, Eq. (34) suggests that above the vector meson production channel and at a fixed production energy, kinematic correlation effects should become increasingly significant for heavier pseudoscalar decay channels.

Second, for a fixed pseudoscalar decay channel, Eq. (34) shows that the kinematic correlation should also become increasingly important with increasing reaction energy owing to the term proportional to $|\mathbf{q}|^2/M_V^2$. In other words, only when the vector meson is produced near threshold (i.e., $|\mathbf{q}|^2/M_V^2 \ll 1$) can the kinematic correlation effects be neglected as a reasonable approximation. Otherwise, uncertainties from such correlations could be substantial.

IV. SUMMARY

We have carried out an analysis of vector meson decay into a pseudoscalar meson plus a photon in photoproduction reactions (e.g., $\omega \to \pi^0\gamma, \phi \to \eta\gamma, \rho \to \pi\gamma$, and $K^* \to K\gamma$). Compared with previous measurements of vector meson decays into pseudoscalars, this channel has the advantage of providing additional dynamical information about the vector meson production mechanism owing to the different spin structures carried by the differential decay distributions.

It was found that kinematic correlations become important in this decay channel in the overall c.m. system. An explicit relation for the correlations between the vector meson rest frame and the overall c.m. system was derived in Eq. (33), which highlighted the kinematic sensitivities of the polarization observables studied in different reactions and different pseudoscalar meson decay channels. It is thus useful for providing guidance for experimental investigation of vector meson photoproduction for the purpose of studying nucleon resonance excitations in polarization reactions.

Although the decay channel $V \to P\gamma$ generally has small branching ratios for most vector mesons, it is relatively large for the ω meson with $b_{\omega\to\pi^0\gamma} = (8.5 \pm 0.5)\%$ [13]. Therefore, for ω meson photoproduction, not only will this channel increase the experimental statistics but it will also provide an independent measurement of polarized beam asymmetry, which can then be compared with the one measured in $\omega \to \pi^0\pi^+\pi^-$. For ϕ and ρ^0, their dominant decays are into two pseudoscalars. Hence, additional spin structure information can be expected in $\phi \to \eta\gamma$ and $\rho^0 \to \pi^0\gamma$. In particular, $br_{\phi\to\eta\gamma} = (1.295 \pm 0.025)\%$ [13] is still sizeable, making this channel an important source for the ϕ meson photoproduction mechanism near threshold. Experimental facilities at ESRF (GRAAL), SPring-8 (LEPS), and ELSA (Crystal Ball) with linearly polarized photon beams and charge-neutral particle detectors should have advantages for addressing this issue.

We also derived the single polarization observables for vector meson photoproduction in terms of the density matrix elements for the polarized particles. Those elements can be directly related to the experimental measurement of the corresponding angular distributions of the vector meson decays into either spinless mesons or a spinless meson plus a photon. For linearly polarized photon beams the angular distribution of the photoproduced vector meson decay into spinless particles has been developed in the literature [10]. Polarization observables in terms of the bilinear helicity product of the helicity amplitudes have also been discussed widely in the literature [9]. In the Appendix, we present the vector meson decay distribution functions in terms of those measurable density matrix elements defined for those polarized particles. This should be useful for future experimental analyses at GRAAL, JLab, and SPring-8, with polarized targets, recoil polarization, or beam-target double polarizations.

ACKNOWLEDGMENTS

This work is supported by the U.K. Engineering and Physical Sciences Research Council Advanced Fellowship (Grant No. GR/S99433/01) and NSF Grant No. PHY-0417679. Q.Z. thanks A. D'Angelo, J.-P. Didelez, E. Hourany, and D. Rebreyend for many useful discussions about the GRAAL experiment.

APPENDIX: DENSITY MATRIX ELEMENTS FOR POLARIZATION OBSERVABLES

In Ref. [10], the density matrix elements for polarized photon beams were derived. We shall adopt the same convention and derive density matrix elements for other single-polarization (i.e., polarized target, recoil polarization, and vector meson polarization) and double-polarization observables. First, we will outline several basic aspects of density matrix elements with polarized photon beams, which will be useful for further discussions.

For the convenience of comparing with other analyses [9], we also express the invariant amplitudes as the following 12 independent helicity amplitudes:

$$\begin{aligned} H_{1\lambda_v} &= \langle \lambda_v, \lambda_f = +1/2 | T | \lambda_\gamma = 1, \lambda_i = -1/2 \rangle, \\ H_{2\lambda_v} &= \langle \lambda_v, \lambda_f = +1/2 | T | \lambda_\gamma = 1, \lambda_i = +1/2 \rangle, \\ H_{3\lambda_v} &= \langle \lambda_v, \lambda_f = -1/2 | T | \lambda_\gamma = 1, \lambda_i = -1/2 \rangle, \\ H_{4\lambda_v} &= \langle \lambda_v, \lambda_f = -1/2 | T | \lambda_\gamma = 1, \lambda_i = +1/2 \rangle. \end{aligned} \tag{35}$$

A. Convention and kinematics

The general form of the angular distribution for the vector meson decay into spinless particles (e.g., $\omega \to \pi^+\pi^-\pi^0$, $\rho^0 \to \pi^+\pi^-$, and $\phi \to K^+K^-$) is

$$\begin{aligned} \frac{dN}{d\cos\theta d\phi} &= W(\cos\theta, \phi) \\ &= \sum_{\lambda_v \lambda_v'} \langle \theta, \phi | M | \lambda_v \rangle \rho_{\lambda_v \lambda_v'}(V) \langle \lambda_v' | M^\dagger | \theta, \phi \rangle, \end{aligned} \tag{36}$$

where M is the vector meson decay amplitude and can be factored as

$$\langle \theta, \phi | M | \lambda_v \rangle = C \sqrt{\frac{3}{4\pi}} D^{1*}_{\lambda_v 0}(\phi, \theta, -\phi). \tag{37}$$

The decay angles, θ and ϕ, are defined as the polar and azimuthal angles, respectively, of the flight direction of one of the decay particles in the vector meson rest frame in the case of two-body decay (e.g., $\rho^0 \to \pi^+\pi^-$, or $\phi \to K^+K^-$). For three-body decay of the vector meson (e.g., $\omega \to \pi^0\pi^+\pi^-$) θ and ϕ denote the polar and azimuthal angles, respectively, of the normal direction of the decay plane. The constant C is independent of λ_v and determined by the vector meson decay width; the Wigner rotation functions D follow the convention of Ref. [15] as defined by Eq. (7).

Consequently, the angular distribution of Eq. (36) can be expressed in terms of the vector meson density matrices $\rho_{\lambda_v\lambda'_v}(V)$:

$$W(\cos\theta,\phi) = \frac{3}{4\pi}\sum_{\lambda_v\lambda'_v} D^{1*}_{\lambda_v 0}(\phi,\theta,-\phi)\rho_{\lambda_v\lambda'_v}(V) \times D^{1}_{\lambda'_v 0}(\phi,\theta,-\phi), \tag{38}$$

where $\rho(V)$ is Hermitian, that is, $\rho_{\lambda_v\lambda'_v}(V) = \rho^*_{\lambda'_v\lambda_v}(V)$. Meanwhile, since $W(\cos\theta,\phi)$ is a linear function of $\rho(V)$, it can be decomposed into a linear combination in terms of the polarization status of the particles.

Equation (38) is general for vector meson decays into spinless particles. The vector meson density matrix element $\rho(V)$ can be related to the polarization status of the initial and final state particles in their spin space via the transition amplitudes $T_{\lambda_v\lambda_f,\lambda_\gamma\lambda_i}$. Therefore, for different polarization reactions with the vector meson decays into spinless particles, $\rho(V)$ is the source containing information about the polarization observables. The angular distribution, as a function of $\rho(V)$, hence provides access to the physics reflected by $\rho(V)$. In experiments, $\rho(V)$ is a quantity that can be derived from the data for vector meson decay distributions, whereas in theory, it can be calculated with dynamical models [17–29].

Since $\rho(V)$ is related to the polarization of the initial and final state particles in their spin space, this is equivalent to saying that for different polarizations of the initial and final state particles there are different density matrix elements that can be measured. In this sense, we are also interested in the number of minimum measurements that can provide the maximum amount of information on the transition mechanisms [9].

In the following; we will first rederive the polarized beam asymmetry in terms of the density matrix elements following Ref. [10] and then derive other polarization asymmetries in terms of the corresponding density matrix elements.

B. Polarized beam asymmetry

Substituting Eq. (14) into (38), we can easily reproduce the results of Ref. [10] and obtain the angular distribution

$$\begin{aligned} W(\cos\theta,\phi,\Phi) = {} & W^0\big(\cos\theta,\phi,\rho^0_{\lambda_v\lambda'_v}\big) - P_\gamma\cos 2\Phi \\ & \times W^1\big(\cos\theta,\phi,\rho^1_{\lambda_v\lambda'_v}\big) - P_\gamma\sin 2\Phi \\ & \times W^2\big(\cos\theta,\phi,\rho^2_{\lambda_v\lambda'_v}\big) + \lambda_\gamma P_\gamma \\ & \times W^3\big(\cos\theta,\phi,\rho^3_{\lambda_v\lambda'_v}\big), \end{aligned} \tag{39}$$

where

$$\begin{aligned} W^0(\cos\theta,\phi,\rho^0) = {} & \frac{3}{4\pi}\Big[\frac{1}{2}\sin^2\theta + \frac{1}{2}(3\cos^2\theta - 1)\rho^0_{00} \\ & - \sqrt{2}\,\mathrm{Re}\,\rho^0_{10}\sin 2\theta\cos\phi \\ & - \rho^0_{1-1}\sin^2\theta\cos 2\phi\Big], \\ W^1(\cos\theta,\phi,\rho^1) = {} & \frac{3}{4\pi}\big[\rho^1_{11}\sin^2\theta + \rho^1_{00}\cos^2\theta \\ & - \sqrt{2}\,\mathrm{Re}\,\rho^1_{10}\sin 2\theta\cos\phi \\ & - \rho^1_{1-1}\sin^2\theta\cos 2\phi\big], \\ W^2(\cos\theta,\phi,\rho^2) = {} & \frac{3}{4\pi}\big[\sqrt{2}\,\mathrm{Im}\;\rho^2_{10}\sin 2\theta\sin\phi \\ & + \mathrm{Im}\;\rho^2_{1-1}\sin^2\theta\sin 2\phi\big], \\ W^3(\cos\theta,\phi,\rho^3) = {} & \frac{3}{4\pi}\big[\sqrt{2}\,\mathrm{Re}\;\rho^3_{10}\sin 2\theta\sin\phi \\ & + \mathrm{Im}\;\rho^3_{1-1}\sin^2\theta\sin 2\phi\big]. \end{aligned} \tag{40}$$

For polarized photon beams, the density matrix element ρ^0 corresponds to the unpolarized photon measurement, ρ^1 and ρ^2 correspond to the linearly polarized photon, and ρ^3 corresponds to the circularly polarized photon. The linearly polarized beam asymmetry then is given by the cross-section differences between polarizing the photons along the x_i axis ($\Phi = 0^\circ$) and the y_i axis ($\Phi = 90^\circ$), which correspond to $\mathbf{P}_\gamma$ along $\mp x_i$, respectively. Similar to Eq. (28), we have

$$\check{\Sigma} \equiv \frac{\bar{W}_\perp(\Phi=90^\circ,\rho) - \bar{W}_\parallel(\Phi=0^\circ,\rho)}{\bar{W}_\perp(\Phi=90^\circ,\rho) + \bar{W}_\parallel(\Phi=0^\circ,\rho)} = P_\gamma\frac{\rho^1_{00} + 2\rho^1_{11}}{\rho^0_{00} + 2\rho^0_{11}}. \tag{41}$$

In terms of the helicity amplitudes this expression can be written as

$$\begin{aligned} \check{\Sigma} = {} & \tfrac{1}{2}\big\{-H^r_{1-1}H^r_{41} - H^i_{1-1}H^i_{41} + H^r_{10}H^r_{40} + H^i_{10}H^i_{40} \\ & - H^r_{11}H^r_{4-1} - H^i_{11}H^i_{4-1} + H^r_{2-1}H^r_{31} + H^i_{2-1}H^i_{31} \\ & - H^r_{20}H^r_{30} - H^i_{20}H^i_{30} + H^r_{21}H^r_{3-1} + H^i_{21}H^i_{3-1}\big\} \\ = {} & \tfrac{1}{2}\langle H|\Gamma^4\omega^A|H\rangle. \end{aligned} \tag{42}$$

This expression is the same as that defined in Ref. [9].

C. Target polarization asymmetry

Proceeding to other single-polarization observables, we shall derive the angular distributions of the vector meson decays into spinless particles and express the polarization observables in terms of the corresponding density matrix elements.

The polarization status of the target is defined as

$$\rho(N) = \tfrac{1}{2}(I_{N_i} + \boldsymbol{\sigma}\cdot\mathbf{P}_{N_i}), \tag{43}$$

where I_{N_i} is the 2×2 unity matrix in the spin space of the target and $\mathbf{P}_{N_i}$ is the polarization vector for the target nucleon. In the coordinates of the initial states, we define $\mathbf{P}_{N_i} \equiv P_{N_i}(\cos\Phi, \sin\Phi, 0)$ for polarizing the initial nucleon within the $x_i y_i$ plane, and $\mathbf{P}_{N_i} \equiv P_{N_i}(0,0,\lambda_i)$ for polarizing

the initial nucleon along z_i, where P_{N_i} is the initial nucleon degree of polarization, and Φ is the angle between the polarization vector of the initial nucleon and the production plane ($x_i z_i$ plane).

The polarized target density matrix elements can be related to the elements of the vector meson decay via the production amplitudes T:

$$\rho_{\lambda_v\lambda_v'}(V) = \frac{1}{N}\sum_{\lambda_f\lambda_\gamma\lambda_i\lambda_i'} T_{\lambda_v\lambda_f,\lambda_\gamma\lambda_i}\rho_{\lambda_i\lambda_i'}(N_i)T^*_{\lambda_v'\lambda_f,\lambda_\gamma\lambda_i'}. \tag{44}$$

Decomposition of the polarization status of the target gives

$$\rho(V) = \rho^0 + \sum_{\alpha=1}^{3} P_{N_i}^{\alpha}\rho^{\alpha}, \tag{45}$$

where ρ^0 denotes the density matrix elements with the unpolarized target, and $\rho^{1,2,3}$ denotes the elements with the target polarized along x_i, y_i, and z_i axes in the initial frame. Explicitly, the elements are given as

$$\begin{aligned}
\rho^0_{\lambda_v\lambda_v'} &= \frac{1}{2N}\sum_{\lambda_f\lambda_\gamma\lambda_i} T_{\lambda_v\lambda_f,\lambda_\gamma\lambda_i}T^*_{\lambda_v'\lambda_f,\lambda_\gamma\lambda_i},\\
\rho^1_{\lambda_v\lambda_v'} &= \frac{1}{2N}\sum_{\lambda_f\lambda_\gamma\lambda_i} T_{\lambda_v\lambda_f,\lambda_\gamma-\lambda_i}T^*_{\lambda_v'\lambda_f,\lambda_\gamma\lambda_i},\\
\rho^2_{\lambda_v\lambda_v'} &= \frac{i}{2N}\sum_{\lambda_f\lambda_\gamma\lambda_i} \hat{\lambda}_i T_{\lambda_v\lambda_f,\lambda_\gamma-\lambda_i}T^*_{\lambda_v'\lambda_f,\lambda_\gamma\lambda_i},\\
\rho^3_{\lambda_v\lambda_v'} &= \frac{1}{2N}\sum_{\lambda_f\lambda_\gamma\lambda_i} \hat{\lambda}_i T_{\lambda_v\lambda_f,\lambda_\gamma\lambda_i}T^*_{\lambda_v'\lambda_f,\lambda_\gamma\lambda_i},
\end{aligned} \tag{46}$$

where $\hat{\lambda}_i = \pm 1$ represents the sign of λ_i.

The vector meson decay distribution depends on the properties of the density matrix elements defined here. Applying the parity conservation relation and the requirement that the density matrix elements be Hermitian, we obtain the matrix elements for $\rho^{\alpha}_{\lambda_v\lambda_v'}$ with $\alpha = 1, 2, 3$, corresponding to the polarization of the initial nucleon spin along x_i, y_i, and z_i. Substituting the elements into Eq. (38), we obtain the vector meson distribution in terms of the different polarization status of the target nucleons:

$$\begin{aligned}
W(\cos\theta,\phi,\Phi) = {} & W^0\big(\cos\theta,\phi,\rho^0_{\lambda_v\lambda_v'}\big)\\
&+ P_{N_i}\cos\Phi W^1\big(\cos\theta,\phi,\rho^1_{\lambda_v\lambda_v'}\big)\\
&+ P_{N_i}\sin\Phi W^2\big(\cos\theta,\phi,\rho^2_{\lambda_v\lambda_v'}\big)\\
&+ \hat{\lambda}_i P_{N_i} W^3\big(\cos\theta,\phi,\rho^3_{\lambda_v\lambda_v'}\big),
\end{aligned} \tag{47}$$

where

$$\begin{aligned}
W^0(\cos\theta,\phi,\rho^0) = \frac{3}{4\pi}\Big[&\frac{1}{2}\sin^2\theta + \frac{1}{2}(3\cos^2\theta - 1)\rho^0_{00}\\
&- \sqrt{2}\,\mathrm{Re}\,\rho^0_{10}\sin 2\theta\cos\phi\\
&- \rho^0_{1-1}\sin^2\theta\cos 2\phi\Big],
\end{aligned}$$

$$\begin{aligned}
W^1(\cos\theta,\phi,\rho^1) = \frac{3}{4\pi}\big[&\sqrt{2}\,\mathrm{Im}\,\rho^1_{10}\sin 2\theta\sin\phi\\
&+ \mathrm{Im}\,\rho^1_{1-1}\sin^2\theta\sin 2\phi\big],\\
W^2(\cos\theta,\phi,\rho^2) = \frac{3}{4\pi}\big[&\rho^2_{11}\sin^2\theta + \rho^2_{00}\cos^2\theta\\
&- \sqrt{2}\,\mathrm{Re}\,\rho^2_{10}\sin 2\theta\cos\phi\\
&- \rho^2_{1-1}\sin^2\theta\cos 2\phi\big],\\
W^3(\cos\theta,\phi,\rho^3) = \frac{3}{4\pi}\big[&\sqrt{2}\,\mathrm{Re}\,\rho^3_{10}\sin 2\theta\sin\phi\\
&+ \mathrm{Im}\,\rho^3_{1-1}\sin^2\theta\sin 2\phi\big],
\end{aligned} \tag{48}$$

where Φ again denotes the angle between the polarization vector of the initial nucleon and the production plane.

As addressed earlier, the corresponding angular distribution of the vector meson decays into pions with the polarized target has the same form as Eq. (38), whereas the density matrix elements represent different dynamical information. In analogy with the polarized photon measurement, the cross sections for polarizing the initial nucleon spin projection along the $\pm y_i$ axis (i.e., $\Phi = \pm 90^\circ$) can be obtained by summing all the events together:

$$\begin{aligned}
\bar{W}_{\uparrow}(\Phi = 90^\circ,\rho) &= \int_{\theta=0}^{\pi}\int_{\phi=0}^{2\pi} d\Omega W^0(\cos\theta,\phi,\rho^0)\\
&\quad + P_{N_i}\int_{\theta=0}^{\pi}\int_{\phi=0}^{2\pi} d\Omega W^2(\cos\theta,\phi,\rho^2)\\
&= \bar{W}^0(\rho^0) + P_{N_i}\bar{W}^2(\rho^2)
\end{aligned} \tag{49}$$

and

$$\bar{W}_{\downarrow}(\Phi = -90^\circ,\rho) = \bar{W}^0(\rho^0) - P_{N_i}\bar{W}^2(\rho^2). \tag{50}$$

The polarized target asymmetry is hence defined as the cross-section differences between these two polarizations:

$$\check{T} \equiv \frac{\bar{W}_{\uparrow}(\Phi=90^\circ,\rho) - \bar{W}_{\downarrow}(\Phi=-90^\circ,\rho)}{\bar{W}_{\uparrow}(\Phi=90^\circ,\rho) + \bar{W}_{\downarrow}(\Phi=-90^\circ,\rho)} = P_{N_i}\frac{\rho^2_{00}+2\rho^2_{11}}{\rho^0_{00}+2\rho^0_{11}}, \tag{51}$$

where P_{N_i} depends only on the experimental setup.

Compared with the polarized beam asymmetry, this equation shows that the density matrix elements $\rho^{1,2,3}$ defined in the target polarization have different properties. In particular, the asymmetry of polarizing the initial nucleon along the x_i axis would be zero if the vector meson decay events are integrated over θ and ϕ.

The dynamic significance can be seen more transparently in terms of the helicity amplitudes, that is,

$$\begin{aligned}
\check{T} &= \sum_{\lambda_v}\left\{H^r_{1\lambda_v}H^i_{2\lambda_v} - H^i_{1\lambda_v}H^r_{2\lambda_v} + H^r_{3\lambda_v}H^i_{4\lambda_v} - H^i_{3\lambda_v}H^r_{4\lambda_v}\right\}\\
&= -\frac{1}{2}\langle H|\Gamma^{10}\omega^1|H\rangle,
\end{aligned} \tag{52}$$

which now involves interferences between different helicity amplitudes and again arrives at the same result as that of Ref. [9].

D. Recoil polarization asymmetry

Similarly, we can also establish the relations for the density matrix elements between the vector meson and the recoil nucleon by defining

$$\rho(N_f) = \tfrac{1}{2}(I_{N_f} + \boldsymbol{\sigma}\cdot\mathbf{P}_{N_f}), \tag{53}$$

where I_{N_f} is the 2×2 unity matrix in the spin space of the recoil nucleon and $\mathbf{P}_{N_f}$ is the polarization direction defined in the final state coordinates [i.e., the frame of (x_f, y_f, z_f) in Fig. 1]. In the spin space for the recoil nucleon, the decomposition of the recoil polarizations leads to

$$\begin{aligned}
\rho^0_{\lambda_v\lambda'_v} &= \frac{1}{2N}\sum_{\lambda_f\lambda_\gamma\lambda_i} T_{\lambda_v\lambda_f,\lambda_\gamma\lambda_i} T^*_{\lambda'_v\lambda_f,\lambda_\gamma\lambda_i},\\
\rho^1_{\lambda_v\lambda'_v} &= \frac{1}{2N}\sum_{\lambda_f\lambda_\gamma\lambda_i} T_{\lambda_v-\lambda_f,\lambda_\gamma\lambda_i} T^*_{\lambda'_v\lambda_f,\lambda_\gamma\lambda_i},\\
\rho^2_{\lambda_v\lambda'_v} &= \frac{i}{2N}\sum_{\lambda_f\lambda_\gamma\lambda_i} \hat{\lambda}_f T_{\lambda_v-\lambda_f,\lambda_\gamma\lambda_i} T^*_{\lambda'_v\lambda_f,\lambda_\gamma\lambda_i},\\
\rho^3_{\lambda_v\lambda'_v} &= \frac{1}{2N}\sum_{\lambda_f\lambda_\gamma\lambda_i} \hat{\lambda}_f T_{\lambda_v\lambda_f,\lambda_\gamma\lambda_i} T^*_{\lambda'_v\lambda_f,\lambda_\gamma\lambda_i},
\end{aligned} \tag{54}$$

where $\hat{\lambda}_f = \pm 1$ represents the sign of λ_f.

The angular distribution of the vector meson decays can then be expressed as

$$\begin{aligned}
W(\cos\theta,\phi,\Phi) = {} & W^0\big(\cos\theta,\phi,\rho^0_{\lambda_v\lambda'_v}\big)\\
&+ P_{N_f}\cos\Phi W^1\big(\cos\theta,\phi,\rho^1_{\lambda_v\lambda'_v}\big)\\
&+ P_{N_f}\sin\Phi W^2\big(\cos\theta,\phi,\rho^2_{\lambda_v\lambda'_v}\big)\\
&+ \hat{\lambda}_f P_{N_f} W^3\big(\cos\theta,\phi,\rho^3_{\lambda_v\lambda'_v}\big),
\end{aligned} \tag{55}$$

where the $W^{0,1,2,3}$ correspond to distributions with the final state baryon unpolarized, polarized along x_f, y_f, and z_f directions, respectively. The expressions of $W^{0,1,2,3}$ are the same as Eq. (48).

Similar to the derivation in previous subsections, the recoil polarization asymmetry is defined as the cross-section differences between polarizing the final-state nucleon along the $\pm y_f$ axis (corresponding to $\Phi = \pm 90^\circ$):

$$\begin{aligned}
\check{P}_{N_f} &\equiv \frac{\bar{W}_\uparrow(\Phi=90^\circ,\rho) - \bar{W}_\downarrow(\Phi=-90^\circ,\rho)}{\bar{W}_\uparrow(\Phi=90^\circ,\rho) + \bar{W}_\downarrow(\Phi=-90^\circ,\rho)}\\
&= P_{N_f}\frac{\rho^2_{00}+2\rho^2_{11}}{\rho^0_{00}+2\rho^0_{11}},
\end{aligned} \tag{56}$$

which is familiar in form to Eq. (51).

Again, in terms of the helicity amplitudes, the dynamic significance can be seen:

$$\begin{aligned}
\check{P}_{N_f} &= \sum_{\lambda_v}\left\{H^i_{3\lambda_v}H^r_{1\lambda_v} - H^r_{3\lambda_v}H^i_{1\lambda_v} + H^i_{4\lambda_v}H^r_{2\lambda_v} - H^r_{4\lambda_v}H^i_{2\lambda_v}\right\}\\
&= \frac{1}{2}\langle H|\Gamma^{12}\omega^1|H\rangle,
\end{aligned} \tag{57}$$

which is the same as that given by Ref. [9].

E. Beam-target double-polarization asymmetry

With the density matrix elements for the photon beams, target nucleon, recoil nucleon, and vector meson, one can proceed to the investigation of double polarizations in terms of the vector meson density matrix elements.

We shall start with the beam-target double polarization, for which experiments will soon be available at GRAAL [7] and JLab [8]. Similar to the single polarizations, the vector meson density matrix elements is related to the polarization status of the photon and target nucleon. Namely, we have

$$\begin{aligned}
\rho(V) &= T\rho(\gamma)\rho(N_i)T^\dagger\\
&= \tfrac{1}{4}T(I_\gamma + \boldsymbol{\sigma}\cdot\mathbf{P}_\gamma)(I_{N_i} + \boldsymbol{\sigma}\cdot\mathbf{P}_{N_i})T^\dagger\\
&= \tfrac{1}{4}T(I_\gamma I_{N_i} + \boldsymbol{\sigma}\cdot\mathbf{P}_\gamma I_{N_i} + I_\gamma\boldsymbol{\sigma}\cdot\mathbf{P}_{N_i}\\
&\quad + \boldsymbol{\sigma}\cdot\mathbf{P}_\gamma\boldsymbol{\sigma}\cdot\mathbf{P}_{N_i})T^\dagger,
\end{aligned} \tag{58}$$

where one can see that the double polarization only involves the last term in the parentheses. This formula tell us that the double polarization eventually provides access to the single polarizations as well.

We introduce the indices α and β for the polarization status of the photon beam and the target nucleon, respectively, and express the B-T polarization as

$$\begin{aligned}
W(\cos\theta,\phi,\rho^{\alpha\beta}) = {} & W^{00}(\cos\theta,\phi,\rho^{00})\\
&+ \sum_{\alpha=1}^{3} P^\alpha_\gamma W^{\alpha 0}(\cos\theta,\phi,\rho^{\alpha 0})\\
&+ \sum_{\beta=1}^{3} P^\beta_{N_i} W^{0\beta}(\cos\theta,\phi,\rho^{0\beta})\\
&+ \sum_{\alpha,\beta=1}^{3} P^\alpha_\gamma P^\beta_{N_i} W^{\alpha\beta}(\cos\theta,\phi,\rho^{\alpha\beta}).
\end{aligned} \tag{59}$$

We shall concentrate on the last term, where both the photon and the target nucleon are polarized. The density matrix elements thus can be expressed as

$$\rho^{\alpha\beta}_{\lambda_v\lambda'_v}(V) = \frac{1}{N}\sum_{\lambda_f\lambda_\gamma\lambda'_\gamma\lambda_i\lambda'_i} T_{\lambda_v\lambda_f,\lambda_\gamma\lambda_i}\rho^\alpha_{\lambda_\gamma\lambda'_\gamma}(\gamma)\rho^\beta_{\lambda_i\lambda'_i}(N_i)T^*_{\lambda'_v\lambda_f,\lambda'_\gamma\lambda'_i}. \tag{60}$$

Given the polarization status of the photon and target nucleon, one can derive the transition elements $\rho^\alpha_{\lambda_\gamma\lambda'_\gamma}(\gamma)$ and $\rho^\beta_{\lambda_i\lambda'_i}(N_i)$ in their spin space. For instance, for the polarization that the photon is linearly polarized along the x axis ($\alpha = 1$) and the target nucleon is polarized along the y axis ($\beta = 2$), we have

$$\rho^{12}_{\lambda_v\lambda'_v}(V) = \frac{i}{4N}\sum_{\lambda_f\lambda_\gamma\lambda_i}\hat{\lambda}_i T_{\lambda_v\lambda_f,-\lambda_\gamma-\lambda_i}T_{\lambda'_v\lambda_f,\lambda_\gamma\lambda_i}, \tag{61}$$

where $\hat{\lambda}_i$ denotes the sign of λ_i.

The angular distribution again gives access to the experimental measurement of the B-T asymmetry in terms of the density matrix elements:

$$\mathcal{C}_{xy}^{\gamma N_i} = \frac{\rho_{00}^{12} + 2\rho_{11}^{12}}{\rho_{00}^{00} + 2\rho_{11}^{00}}, \tag{62}$$

which has the same form as other single polarizations; ρ_{00}^{00} and ρ_{11}^{00} denote the unpolarized density matrix elements and $\rho_{00}^{00} + 2\rho_{11}^{00} = 1$ owing to the normalization. Undoubtedly, the dynamic information is contained in the helicity products selected by the polarization status, and again, the B-T polarization experiment will pick up the double-polarization asymmetry:

$$\begin{aligned}\mathcal{C}_{xy}^{\gamma N_i} &= -\frac{i}{2}\{H_{11}^* H_{3-1} + H_{21}^* H_{4-1} - H_{31}^* H_{1-1} - H_{41}^* H_{2-1} \\ &\quad + H_{1-1}^* H_{31} + H_{2-1}^* H_{41} - H_{3-1}^* H_{11} - H_{4-1}^* H_{21} \\ &\quad - H_{10}^* H_{30} - H_{20}^* H_{40} + H_{30}^* H_{10} + H_{40}^* H_{20}\} \\ &= -\frac{1}{2}\sum_{a,b,\lambda_v,\lambda_v'} H_{a\lambda_v}^* \Gamma_{ab}^{12} \omega_{\lambda_v\lambda_v'}^{A} H_{b\lambda_v'},\end{aligned} \tag{63}$$

which is the same as defined in Ref. [9] and Γ_{ab}^{12} and $\omega_{\lambda_v\lambda_v'}^{A}$ are 4×4 and 3×3 Hermitian matrices, respectively.

[1] F. J. Klein (SAPHIR Collaboration), PiN Newslett. **14**, 141 (1998).

[2] Y. Assafiri *et al.* (GRAAL Collaboration), in *Proceedings of NSTAR 2002 Workshop on the Physics of Excited Nucleons, Pittsburgh, 2002*, edited by S. A. Dytman and E. S. Swanson (World Scientific, River Edge, N.J.), p. 261; A. D'Angelo *et al.* (GRAAL Collaboration), in *Proceedings of 9th International Conference on the Structure of Baryons, 2002*, Newport News, edited by C. E. Carlson and B. A. Mecking (World Scientific, N.J.), p. 140.

[3] P. Ambrozewicz *et al.* (Jefferson Laboratory E91-016 Collaboration), Phys. Rev. C **70**, 035203 (2004).

[4] V. D. Burkert, submitted to Int. J. Mod. Phys. A [arXiv:nucl-ex/0412033].

[5] N. Isgur and G. Karl, Phys. Lett. **B72**, 109 (1977); Phys. Rev. D **18**, 4187 (1978); **19**, 2653 (1979) [Erratum, **23**, 817 (1981)]; R. Koniuk and N. Isgur, Phys. Rev. D **21**, 1868 (1980) [Erratum **23**, 818 (1981)].

[6] S. Capstick and W. Roberts, Prog. Part. Nucl. Phys. **45**, 5241 (2000).

[7] S. Bouchigny *et al.*, in *Proceedings of International Symposium on Electromagnetic Interactions in Nuclear and Hadron Physics (EMI 2001), Osaka, Ibaraki, Japan, 2001*, edited by M. Fujiwara and T. Sinha (World Scientific, Singapore), p. 688.

[8] P. L. Cole *et al.*, in *Proceedings of International Symposium on Electromagnetic Interactions in Nuclear and Hadron Physics (EMI 2001), Osaka, Ibaraki, Japan, 2001*, edited by M. Fujiwara and T. Sinha (World Scientific, Singapore), p. 652.

[9] M. Pichowsky, C. Savklı, and F. Tabakin, Phys. Rev. C **53**, 593 (1996).

[10] K. Schilling, P. Seyboth, and G. Wolf, Nucl. Phys. **B15**, 397 (1970).

[11] W. M. Kloet and F. Tabakin, Phys. Rev. C **61**, 015501 (2000).

[12] W. M. Kloet, W. T. Chiang, and F. Tabakin, Few Body Syst. Suppl. **11**, 308 (1999).

[13] S. Eidelman *et al.* (Particle Data Group), Phys. Lett. **B592**, 1 (2004).

[14] C. Becchi and G. Morpurgo, Phys. Rev. B **140**, 687 (1965).

[15] M. E. Rose, *Elementary Theory of Angular Momentum* (Wiley, New York, 1957).

[16] Q. Zhao, Phys. Rev. C **63**, 025203 (2001); in *Proceedings of the International Symposium on Electromagnetic Interactions in Nuclear and Hadron Physics (EMI2001), Osaka, Japan, 2001*, edited by M. Fujiwara and T. Sinha (World Scientific, Singapore), p. 632.

[17] Q. Zhao, Z. Li, and C. Bennhold, Phys. Lett. **B436**, 42 (1998); Phys. Rev. C. **58**, 2393 (1998).

[18] B. Friman and M. Soyeur, Nucl. Phys. **A600**, 477 (1996).

[19] Q. Zhao, J. S. Al-Khalili, and C. Bennhold, Phys. Rev. C **64**, 052201(R) (2001).

[20] Q. Zhao, B. Saghai, and J. S. Al-Khalili, Phys. Lett. **B509**, 231 (2001).

[21] A. I. Titov, M. Fujiwara, and T. S. H. Lee, Phys. Rev. C **66**, 022202(R) (2002).

[22] A. I. Titov and T. S. H. Lee, Phys. Rev. C **66**, 015204 (2002); **67**, 065205 (2003).

[23] Y.-s. Oh, A. Titov, and T. S. H. Lee, Phys. Rev. C **63**, 025201 (2001).

[24] A. I. Titov, Y.-s. Oh, S. N. Yang, and T. Morii, Phys. Rev. C **58**, 2429 (1998).

[25] Y.-s. Oh and T. S. H. Lee, Phys. Rev. C **66**, 045201 (2002); **69**, 025201 (2004).

[26] Y.-s. Oh and H. C. Bhang, Phys. Rev. C **64**, 055207 (2001).

[27] V. Shklyar, H. Lenske, U. Mosel, and G. Penner, submitted to Phys. Rev. C [arXiv:nucl-th/0412029].

[28] G. Penner and U. Mosel, Phys. Rev. C **66**, 055211 (2002); **66**, 055212 (2002).

[29] T. Feuster and U. Mosel, Phys. Rev. C **59**, 460 (1999).